POLITECNICO DI TORINO
Repository ISTITUZIONALE

Ground currents in a photovoltaic power plant: Theoretical approach and experimental tests

(Article begins on next page)

03 October 2022

Ground Currents in a Photovoltaic Power Plant: Theoretical Approach and Experimental Tests

Alessandro Ciocia*, Valeria Cocina†, Pietro Colella*,
Paolo Di Leo*, Enrico Pons*, Filippo Spertino*, Riccardo Tommasini*
* Dipartimento Energia, Politecnico di Torino, Torino, 10129, Italy
† Edilizia e Logistica, Politecnico di Torino, Torino, 10129, Italy
Email: pietro.colella@polito.it

Abstract—**Arrays of photovoltaic (PV) modules, mounted on metallic structures, always create stray capacitances between active conductors and ground. Thus, leakage currents flowing in these ground capacitances are formed. If the number of PV modules array is high, these currents can reach some amperes. Noticeable leakage currents can cause several problems related to the proper operation of electrical installation and appliances and to the safety of people. In this work, the problem of the ground currents in PV arrays is firstly studied from a theoretical point of view. Suitable equivalent circuits are presented. Then, the set-up and the results of a field measurement for the estimation of the leakage currents in an operating PV power plant are reported.**

Index Terms—**Photovoltaic systems, field measurement, ground capacitance, leakage current.**

I. INTRODUCTION

In the last decades, grid connected photovoltaic (PV) systems have become increasingly important in distributed power generation. Together with governmental incentives, key elements for this success have been PV systems efficiency improvement and their installation cost reduction, which have been possible thanks also to an innovative interconnection scheme: if in the past most PV systems were interconnected to the grid trough a low-frequency transformer, nowadays a transformerless solution is recommended.

In the latter case, in fact, the transformer cost is avoided and the PV generation system is characterized by a higher efficiency, a smaller size and weight [1].

Unfortunately, some negative aspects are associated to this interconnection method, because the galvanic isolation between the PV system and the grid, that was guaranteed by the transformer, is no more ensured. An AC leakage current can now flow through inverter, ground and stray capacitances C_S formed by the PV module electrically active layers and the surrounding metallic structures. In particular, positive and negative terminals with respect to the aluminum frame of PV modules determine charge accumulation. The higher the capacitances, the higher the leakage current, which is then function of several parameters, such as the module surfaces, the distance between the active parts and metallic structures, and the nature of the insulation material [1], [2].

The effects of the leakage current are several; for example, it can increase the inverter losses and cause electromagnetic interference [3], [4]. Its suppression or limitation is particularly

important in environments with an explosive atmosphere, where fires and explosions could be triggered.

In order to detect and remove dangerous leakage currents, The International Standard IEC 62109-2:2011 requires the installation of a Residual Current Device (RCD) or a Residual Current Monitoring Unit (RCMU), which can be embedded or be external to the inverter [3], [5]. If the leakage current is remarkable, the RCD tripping threshold can be easily reached, with the consequent disconnection of the PV power plant and, then, economical losses.

Based upon these safety and economical reasons, it is clear that the reduction of the leakage currents is an important objective. According to this, several techniques have been proposed in literature [3], [6]; basically, they can be categorized in three different groups: modulation solutions [7], [8], topology solutions [8]–[10] and filter solutions [11].

Furthermore, the comparison and analysis of transformerless grid connected PV inverter topologies and control strategies have been carried out in many manuscripts [12], [13].

The main goal of this work is to evaluate the leakage current that flows to ground in a real PV grid-connected power system. In the following sections, the circuital model of the grid-connected PV system is introduced (section II); then, the structure of the system under test is described and the measurement results are presented (section III). Finally, the main conclusions of the work are reported (section IV).

II. LEAKAGE CURRENT IN A GRID CONNECTED PV SYSTEM: CIRCUITAL MODEL

In order to understand how a ground current can be generated, a circuital scheme of a three phase transformerless PV power plant is reported in Fig. 1. In the following paragraphs, each block is shortly described.

A. PV Module

The cross-section of a typical PV module is depicted in Fig. 2 [14]. The PV cells are kept in place by a transparent encapsulant material (usually ethyl vinyl acetate, EVA); on the front side they are protected by a transparent layer: low iron-content tempered glass is the most common choice as it is low cost, strong, stable and highly transparent; on the back, except in bi-facial modules, a thin polymer sheet, normally
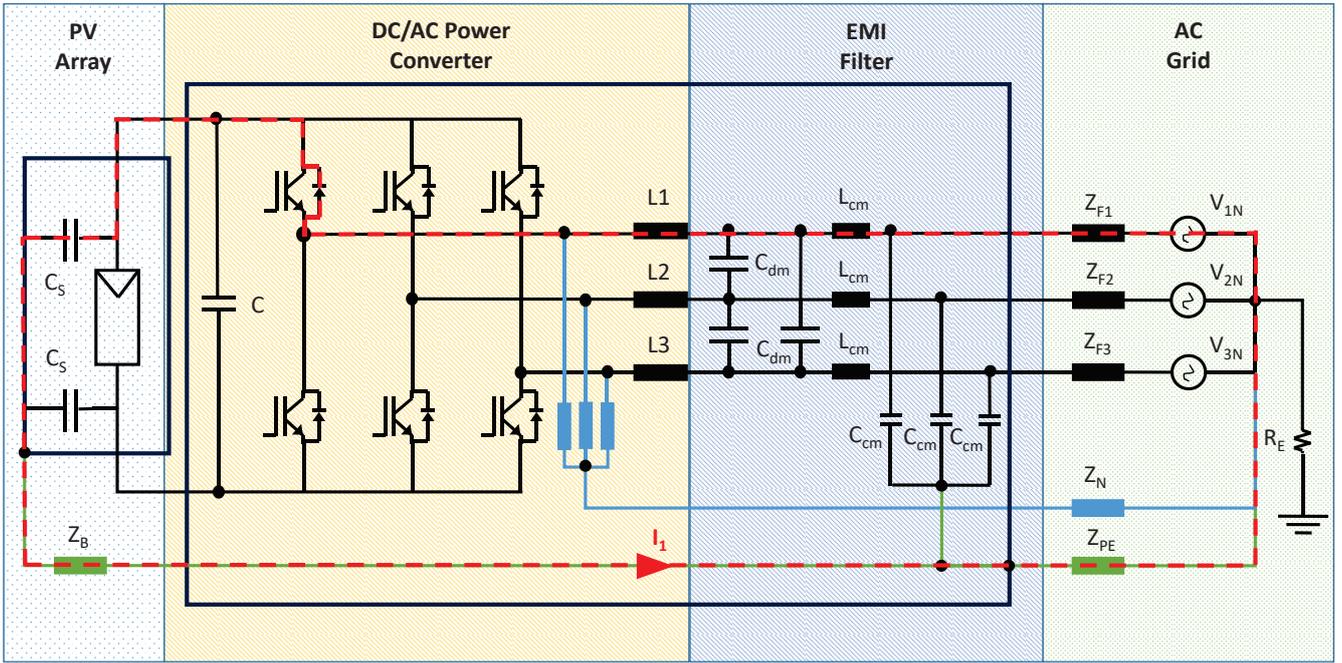
Fig. 1. Circuital scheme of a PV transformerless power plant and current path through the stray capacitances.
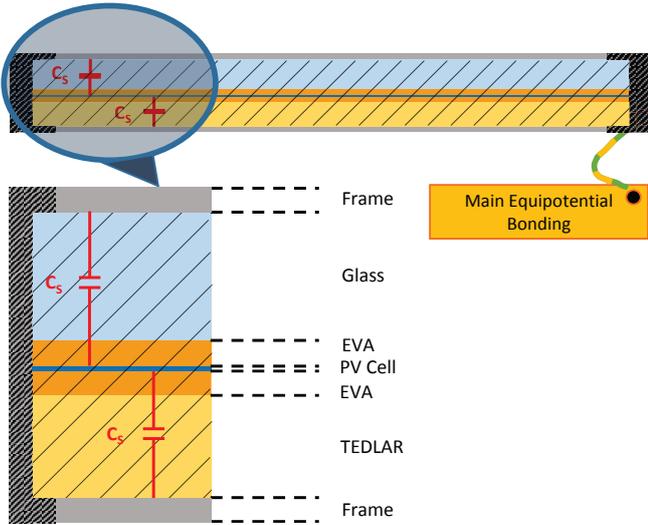

Fig. 2. Cross-section of a typical PV module.

Tedlar, is used. An important structural element, that allows anchoring the PV modules, is the frame, usually in aluminum. As shown, the proximity of insulating and conductive layers in the PV module forms stray capacitances between positive and negative terminals with respect to the aluminum frame.

In the "PV Array block" (Fig. 1), the stray capacitances are represented and indicated as C_S. In the considered circuit, the metallic framework is connected to ground through the bonding conductor characterized by the impedance Z_B. It is important to specify that this interconnection is not always

implemented.

B. DC/AC Power Converter

In order to describe the problem of the ground leakage current, a standard inverter topology was chosen. In the considered inverter (Fig. 1), the DC link is formed by the two capacitors C. This configuration provides the medium point M of the DC bus.

Moreover, on the AC side, the neutral point N can be derived. According to the design of the inverter, the points N and M can be interconnected to ground or floating, they can be connected together or not. These choices influence the value of the ground current.

$L1$, $L2$, $L3$ are the output coupling inductances for the control of the current injected into the grid. They have an effect similar to that of the stator winding inductances of a synchronous generator.

C. EMI Filter

The Electromagnetic Compatibility (EMC) is one of the aspects to be reckoned in the DC/AC converters. In general, EMC means the ability of an electrical device to function correctly in the electromagnetic environment in which it is inserted, without causing or being subject to interferences with the electric and magnetic fields, due to voltage and current variations which arise within the device.

EMC aims to examine both the conditions under which the electrical devices retain their functionality in presence of external disturbances (in particular of electromagnetic nature) and the level of emitted interferences which may affect other devices operating in the same environment.

Electromagnetic interferences can appear in the form of voltage component and current component of common mode (CM), asymmetric, and differential mode (DM), symmetric. In the DM, the current component flows in the power lines (including the neutral line), while the voltage component is measured between the phase conductors. On the contrary, in the CM the current component flows between the phase and neutral conductors to the ground. The circuit for the CM component is closed by the parasitic capacitances between the ground and the circuit.

The EMC problems, both CM and DM, can be solved with the use of EMI (Electromagnetic Interference) filters able to reduce natural or technical interferences. Generally, in grid-connected PV systems two EMI filters can be used: one in input to block (or limit) the high frequency components coming from the PWM inverter and one in output to limit the EMI produced by the electric power system itself.

Generally, it is necessary to arrange filters which are transparent to the AC voltage at 50Hz and allow a reduction of the interference level, in order to meet the requirements imposed by IEC Standards. According to this, an EMI filter can be considered a low-pass filter.

In Fig. 1, the components of a typical EMI filter are depicted [7]:

- C_{dm} are the differential mode capacitors;
- L_{cm} are the common mode inductors;
- C_{cm} are the common mode capacitors.

D. AC Grid

In this work, only PV power plants installed in TN-S systems are considered.

In the "AC Grid" block in Fig. 1, the portion of the distribution system between the secondary windings of the transformer and the switchboard of the inverter is modeled.

In particular:

- Z_{F1}, Z_{F2}, Z_{F3} are the impedances of the phase conductors;
- Z_N is the impedance of the neutral conductor;
- Z_{PE} is the impedance of the protective conductor (PE);
- V_{1N}, V_{2N}, V_{3N} are the voltages imposed by the transformer with reference to its neutral point;
- R_E is the resistance to earth of the grounding system [15].

E. Path of the Ground Current through the Stray Capacitances

The ground currents can be generated by the grid voltage sources and the PWM inverter. In this work, the PWM inverter components from triangular carrier are not of interest because they produce negligible harmonic components in the ground current.

In Fig. 1, the red dashed line represents one of the possible paths of the leakage current through the stray capacitances.

In particular, starting from the neutral point of the transformer, the current flows through the cables of the phase 1, the freewheeling diode, the PV stray capacitances and it returns to the generator through the bonding and protective conductors.

In this circuit, the voltage that sustains the leakage current is V_{1N}, while the dominant impedance is $Z = \dfrac{1}{\omega C_S}$.

Similar paths can be defined for each of the other voltage sources in the electrical circuit and for each of the freewheeling diodes of the inverter.

III. EXPERIMENTAL MEASUREMENT

A measurement campaign has been organized in order to gain experimental evidence of the ground leakage current in a practical case. In the following paragraphs, the PV power plant where the measurements have been carried out, the experimental set-up and the measurement results are briefly described.

A. The PV power plant

The grid-connected PV system, located at latitude $45.065°$ North (Piedmont region), has a total power rating $P_{peak} = 600.372\ kWp$ at Standard Test Conditions (STC), i.e. global irradiance $G_{STC} = 1\ kW/m^2$, cell temperature $T_{STC} = 25°C$ and standard spectrum $AM\ 1.5$.

Due to design requirements, the realization of the PV plant has been divided into 2 parts with approximately half of the P_{peak} each: the first one was installed in 2015; the second one has been completed in 2016.

The PV system is equipped with mono-crystalline silicon modules of $327\ Wp$ each, tilted at $26°$ with South orientation. The PV arrays of each part feed 14 three-phase inverters with high efficiency (transformerless type) of $20\ kVA$ or $25\ kVA$.

The modules are installed on a portion of the roof, by means of an aluminum framework, Fig. 3. All the surrounding metallic structures of the PV modules are interconnected to ground through mainly two paths: first, through several bonding and protective conductors, as visible in Fig. 3; second, through the roof on which the aluminum framework is bolted, that is metallic with the exception of the exterior surface. The low impedance of these paths was verified with continuity tests.

B. Experimental setup

In order to measure the waveform of ground currents during the operation of a PV system in grid connection, it is advisable to use an appropriate automatic data acquisition system (ADAS). It consists of:

- current/voltage probes;
- signal conditioning circuit;
- Sample/Hold (S/H) with multiplexer stage;
- Analogue-Digital Converter (ADC).

Voltage probes permit to extend the voltage ranges from a few volts in DC to $\pm1000\ V$ in both DC and AC. On the other hand, a Hall-effect current probe permits to convert signals up to $\pm2000\ A$ in both DC and AC into low-range voltage signals of $\pm1\ V$.

The signal conditioning circuit, thanks to divider and amplifier ratios, modifies the input signal into an output signal as close as possible to the proper range of the ADC.

Fig. 3. PV modules, aluminum frameworks and bonding conductors.

Fig. 4. Single inverter and total ground leakage current measurement.

Fig. 5. Single inverter and total current waveforms.

The main specifications of the ADC, usually a successive approximation converter, are: the maximum sampling rate in MSa/s and the related frequency range; the number of bits which determines the resolution (16 bits are enough). Taking into account the previous items, the ADAS capabilities can be expressed in terms of measurement uncertainties on AC voltage and AC current within a frequency range.

If the case study of the ground currents is considered, relative uncertainties are normally within $\pm 0.1\%$ for voltage and $\pm 1\%$ for current in a three-phase PV system in grid connection without interface transformer. The frequency range should include the PWM harmonic content of the inverter and thus 20 kHz could be an acceptable superior limit.

C. Measurement results and discussion

In order to have both a general and a particular point of view of the phenomenon, two ground leakage currents were measured: I_{SI}, the leakage of a single inverter for which the conductors were easily accessible, and I_{TC}, the total leakage of all the inverters connected to the same switchboard (14 in our test case). Both currents have been measured as the sum of currents flowing in the three phase conductors and in the neutral conductor, by clamping all four conductors at the same time with the current probe (Fig. 4). With this connection of the current clamps, leakage currents have been measured like a RCD would do. They have not been measured by clamping directly the PE, as this would lead to erroneous readings: multiple re-closure paths for the leakage currents can, in fact, be present in the circuit.

In addition to currents measurements, in order to have a phase reference, the amplitude and the phase of voltages V_{1N}, V_{2N} and V_{3N} were also measured.

Two periods of the single inverter and of the total ground leakage currents are presented in Fig. 5 as an example.

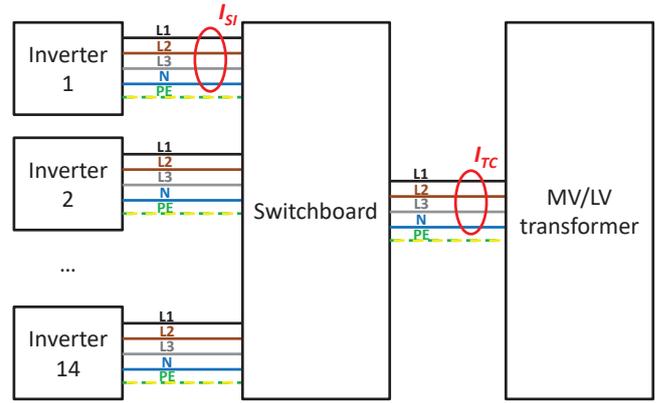The registered waveforms were then processed to obtain the equivalent phasor representation. In particular, the measured signals were decomposed using the FFT (Fast Fourier Transform). The frequency domain representation of the considered currents is reported in Fig. 6. With reference to the I_{TC}, the 50 Hz component has clearly the largest RMS value. On the contrary, for the I_{SI}, the DC and 50 Hz components are comparable, probably due to a non-perfect reset to zero of the current probe. However, in this analysis, only the 50 Hz component was considered.
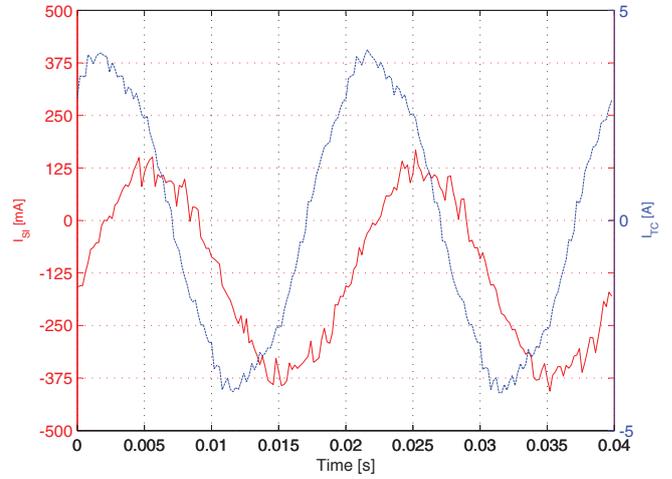
For a better comprehension of the phenomenon, in addition to the measured currents and voltages, the zero-sequence voltage E_0 was computed [16]:

$$E_0 = \frac{V_{1N} + V_{2N} + V_{3N}}{3} \quad (1)$$

This voltage can be considered the feeding source of the current flowing through the ground.

The RMS value of the current I_{SI}, which flows through one single inverter, is 0.18 A. The RMS value of the current I_{TC}, which is the vectorial sum of the currents leaked through all the inverters, is 2.76 A. This means, as the number of inverters is 14, that the leakage currents of all the inverters are
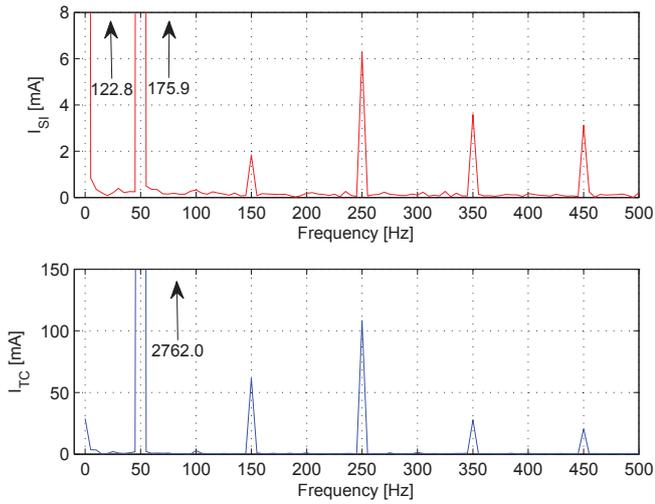
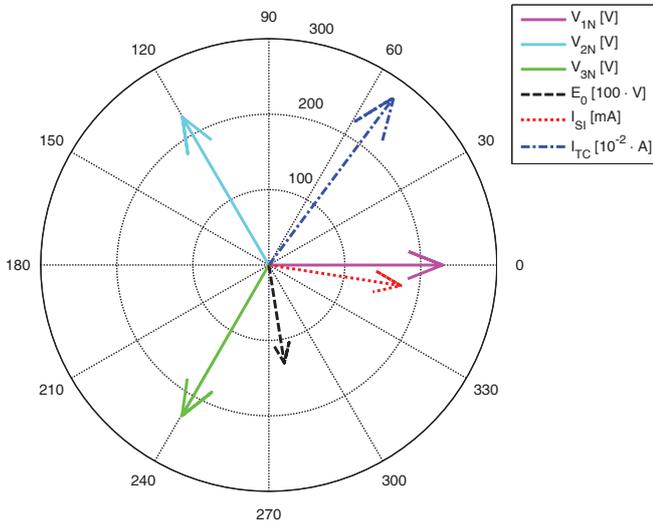Fig. 6. Frequency domain representation of the currents measured (RMS).

Fig. 7. Polar representation of the RMS currents and voltages phasors.

approximately in phase. This leakage current is not negligible: in this case study there are no problems, however, if the PV arrays are installed in higher risk environments, such as where combustible dusts or gases can be present, particular attention should be paid to this problem in order to avoid risk of fire or explosion [17]. Moreover, in order to avoid the disconnection of the PV power plant, the tripping threshold of the RCD should be higher than the measured leakage current, with a consequent reduction of the safety against electric shocks. In this PV plant, the RCD protecting the single inverter was not triggered, as it had a rated residual current of $300\ mA$; on the contrary, in the MV/LV substation RCDs were not present, as permitted in TN systems.

A polar representation of the currents and voltages phasors is reported in Fig. 7.

It can be noticed that both the currents I_{TC} and I_{SI} lead the voltage E_0 by 73° and 134°, respectively. This is due to the characteristics of the electrical circuit described in paragraph II-E, where the stray capacitances C_S play a key role.

IV. CONCLUSION

In this paper, the problem of ground leakage currents in arrays of photovoltaic modules, due to PV stray capacitances, is presented with experimental results. It can cause several issues, such as an increment of the inverter losses, electromagnetic disturbances and a reduction of safety. In fact, in environments where an explosive atmosphere can be present, it can cause fire or explosions. In addition, it forces electrical designers to increase the tripping threshold of residual current devices to avoid the disconnection of the PV plant, thus increasing the risk of electric shock. The suppression of the leakage current is, therefore, an important objective to be pursued.

In order to quantify the magnitude of this current, field measurements on a real PV system were carried out. The currents flowing through each and every inverters of a multi-inverter PV system were measured with current clamps connected to an automatic data acquisition system. The measurement results show that the total leakage current reached nearly $3\ A$.

Looking at the schematic presented in this paper, one could think to disconnect the metallic frame of PV modules from the PE in order to reduce the leakage current. For class II PV modules, this could be possible, as the metallic frame is not an exposed conductive part. However, the disconnection would not necessarily lead to a significant reduction in leakage current: for example in the PV plant where the measurements were performed, the aluminum frames were in good electrical contact with the metallic roof due to the mounting structure.

The reduction of leakage current should thus be obtained through proper design of the inverter topology and control. It should also be a parameter highlighted by the manufacturers in the data sheets.

REFERENCES

[1] T. Kerekes, M. Liserre, R. Teodorescu, C. Klumpner, and M. Sumner, "Evaluation of three-phase transformerless photovoltaic inverter topologies," *Power Electronics, IEEE Transactions on*, vol. 24, no. 9, pp. 2202–2211, 2009.

[2] T. Tran-Quoc, H. Colin, C. Duvauchelle, B. Gaiddon, C. Kieny, C. L. T. Minh, S. Bacha, S. Aissanous, G. Moine, and Y. Tanguy, "Transformerless inverters and RCD: whats the problem?" in *25th European Photovoltaic Solar Energy Conference and Exhibition/5th World Conference on Photovoltaic Energy Conversion*, 2010, pp. 4554–4559.

[3] R. S. Figueredo, K. C. M. de Carvalho, N. R. N. Ama, and L. Matakas, "Leakage current minimization techniques for single-phase transformerless grid-connected pv invertersan overview," in *2013 Brazilian Power Electronics Conference*. IEEE, 2013, pp. 517–524.

[4] M. Calais, J. Myrzik, T. Spooner, and V. G. Agelidis, "Inverters for single-phase grid connected photovoltaic systems-an overview," in *Power Electronics Specialists Conference, 2002. pesc 02. 2002 IEEE 33rd Annual*, vol. 4. IEEE, 2002, pp. 1995–2000.

[5] *Safety of power converters for use in photovoltaic power systems - Part 2: Particular requirements for inverters*. IEC 62109-2, 2011.

[6] Y. Zhou and H. Li, "Analysis and suppression of leakage current in cascaded-multilevel-inverter-based pv systems," *IEEE Transactions on Power Electronics*, vol. 29, no. 10, pp. 5265–5277, 2014.

[7] E. Gubia, P. Sanchis, A. Ursua, J. Lopez, and L. Marroyo, "Ground currents in single-phase transformerless photovoltaic systems," *Progress in photovoltaics: research and applications*, vol. 15, no. 7, pp. 629–650, 2007.

[8] H. Xiao and S. Xie, "Leakage current analytical model and application in single-phase transformerless photovoltaic grid-connected inverter," *IEEE Transactions on Electromagnetic Compatibility*, vol. 52, no. 4, pp. 902–913, 2010.

[9] M. Poliseno, R. A. Mastromauro, and M. Liserre, "Transformer-less photovoltaic (pv) inverters: A critical comparison," in *2012 IEEE Energy Conversion Congress and Exposition (ECCE)*.   IEEE, 2012, pp. 3438–3445.

[10] B. Yang, W. Li, Y. Gu, W. Cui, and X. He, "Improved transformerless inverter with common-mode leakage current elimination for a photovoltaic grid-connected power system," *IEEE transactions on power electronics*, vol. 27, no. 2, pp. 752–762, 2012.

[11] D. Dong, F. Luo, D. Boroyevich, and P. Mattavelli, "Leakage current reduction in a single-phase bidirectional ac–dc full-bridge inverter," *IEEE Transactions on Power Electronics*, vol. 27, no. 10, pp. 4281–4291, 2012.

[12] T. K. S. Freddy, N. A. Rahim, W.-P. Hew, and H. S. Che, "Comparison and analysis of single-phase transformerless grid-connected pv inverters," *IEEE Transactions on Power Electronics*, vol. 29, no. 10, pp. 5358–5369, 2014.

[13] D. Kumar, A. Pattanaik, and S. Singh, "Comparative assessment of leakage current in a photovoltaic grid connected single phase transformerless inverter system," in *Recent Advances and Innovations in Engineering (ICRAIE), 2014*.   IEEE, 2014, pp. 1–7.

[14] F. Spertino, A. DAngola, D. Enescu, P. Di Leo, G. V. Fracastoro, and R. Zaffina, "Thermal–electrical model for energy estimation of a water cooled photovoltaic module," *Solar Energy*, vol. 133, pp. 119–140, 2016.

[15] *International Electrotechnical Vocabulary - Part 195: Earthing and Protection of Electric Shock*.   IEC 60050-195, 08 1998.

[16] *Short-circuit currents in three-phase a.c. systems - Part 0: calculation of short circuit currents*.   IEC 60909-0, 2001.

[17] R. Tommasini, E. Pons, and F. Palamara, "Area classification for explosive atmospheres: Comparison between european and north american approaches," *IEEE Transactions on Industry Applications*, vol. 50, no. 5, pp. 3128–3134, 2014.